JGP Journal of General Physiology

RESEARCH ARTICLE

PLC and IP_3-evoked Ca^{2+} release initiate the fast block to polyspermy in *Xenopus laevis* eggs

Katherine L. Wozniak, Maiwase Tembo, Wesley A. Phelps, Miler T. Lee, and Anne E. Carlson

The prevention of polyspermy is essential for the successful progression of normal embryonic development in most sexually reproducing species. In external fertilizers, the process of fertilization induces a depolarization of the egg's membrane within seconds, which inhibits supernumerary sperm from entering an already-fertilized egg. This fast block requires an increase of intracellular Ca^{2+} in the African clawed frog, *Xenopus laevis*, which in turn activates an efflux of Cl^- that depolarizes the cell. Here we seek to identify the source of this intracellular Ca^{2+}. Using electrophysiology, pharmacology, bioinformatics, and developmental biology, we explore the requirement for both Ca^{2+} entry into the egg from the extracellular milieu and Ca^{2+} release from an internal store, to mediate fertilization-induced depolarization. We report that although eggs express Ca^{2+}-permeant ion channels, blockade of these channels does not alter the fast block. In contrast, insemination of eggs in the presence of Xestospongin C—a potent inhibitor of inositol 1,4,5-trisphosphate (IP_3)-induced Ca^{2+} release from the endoplasmic reticulum (ER)—completely inhibits fertilization-evoked depolarization and increases the incidence of polyspermy. Inhibition of the IP_3-generating enzyme phospholipase C (PLC) with U73122 similarly prevents fertilization-induced depolarization and increases polyspermy. Together, these results demonstrate that fast polyspermy block after fertilization in *X. laevis* eggs is mediated by activation of PLC, which increases IP_3 and evokes Ca^{2+} release from the ER. This ER-derived Ca^{2+} then activates a Cl^- channel to induce the fast polyspermy block. The PLC-induced cascade of events represents one of the earliest known signaling pathways initiated by fertilization.

Introduction

Embryonic development is a tightly regulated series of events that begins with the fertilization of an egg by a single sperm. This remarkable process of gamete unification is surprisingly error prone. For example, the fertilization of an egg by more than one sperm, a condition known as polyspermy, is a significant barrier to successful reproduction (Wong and Wessel, 2006). Polyspermy causes chromosomal abnormalities that are embryonically lethal in nearly all sexually reproducing species. To avoid polyspermy-induced lethality, eggs have developed multiple mechanisms to prevent sperm entry into an already-fertilized egg (Stricker, 1999; Wong and Wessel, 2006); however, the molecular pathways driving these events are still poorly understood.

The two most common strategies for preventing polyspermy are the fast block and the slow block (Wong and Wessel, 2006). As their names imply, these mechanisms differ with respect to how quickly they occur. The fast block involves depolarization of the egg and occurs within seconds of fertilization (Jaffe, 1976). Cross-species fertilization experiments demonstrated that sperm possess a voltage sensor that prevents their entry into a depolarized egg (Jaffe et al., 1983a). The mechanism that enables sperm to detect the egg's membrane potential remains unknown. In contrast, the slow block involves the creation of a physical barrier surrounding the nascent zygote and takes several minutes to complete (Stricker, 1999; Wong and Wessel, 2006). Whereas the slow block occurs in nearly all sexually reproducing species, the fast block is limited to externally fertilizing organisms in which the sperm-to-egg ratio can be extremely high (Jaffe, 1976; Cross and Elinson, 1980; Jaffe et al., 1983b).

The fast block has been documented in diverse externally fertilizing organisms (Jaffe and Gould, 1985), including fucoid algae (Brawley, 1991), sea urchins (Jaffe, 1976), starfish (Miyazaki and Hirai, 1979), marine worms (Gould-Somero et al., 1979), and amphibians (Cross and Elinson, 1980; Charbonneau et al., 1983). The signaling pathways underlying the fast block remain elusive for most species. Because of evolutionary distance and differences in habitat among the species that use the fast block, the precise mechanisms are likely to vary. Nevertheless, eggs capable of undergoing the fast block share three characteristics: their fertilization-activated membrane depolarization, known as the fertilization potential, persists for 1 min or more (Jaffe, 1976; Grey

Department of Biological Sciences, University of Pittsburgh, Pittsburgh, PA.

Correspondence to Anne E. Carlson: acarlson@pitt.edu.

Table 1. **Biophysical properties of the fertilization-evoked depolarizations**

	Resting potential	Fertilization potential	Sperm addition to depolarization time	Depolarization rate	*n*
	mV	*mV*	*min*	*mV/ms*	
Control (MR/5)	−17.9 ± 0.9	−2.6 ± 1.2	5.3 ± 0.5	3.9 ± 0.8	31
10 µM $GdCl_3$	−17.0 ± 2.3	−2.6 ± 0.7	3.5 ± 0.8	10.6 ± 7.9	8
20 µM SK&F-96365	−13.6 ± 2.0	−6.4 ± 1.9	3.8 ± 1.0	6.1 ± 3.6	6
500 nM Xestospongin C	−11.0 ± 1.4	—	—	—	5
2% DMSO	−21.5 ± 4.2	−6.6 ± 2.3	8.0 ± 1.4	5.8 ± 3.4	5
100 µM 2-APB	−19.6 ± 1.4	−4.8 ± 2.0	6.6 ± 1.8	0.6 ± 0.3	8
1 µM U73122	−22.1 ± 4.1	—	—	—	7
1 µM U73343	−20.8 ± 2.3	−3.7 ± 1.2	1.9 ± 0.4	14.9 ± 6.6	8

Mean ± SEM for the indicated measurement before, during, and after the fertilization-signaled depolarization.

et al., 1982), thereby distinguishing it from action potentials in other excitable cells such as neurons or cardiac myocytes (Hille, 2001); when held at their fertilization potential voltage, the eggs can be bound, but not entered, by sperm (Jaffe, 1976); and when held at hyperpolarized potentials, the eggs can be fertilized by multiple sperm (Jaffe, 1976).

A Cl^- current depolarizes frog eggs at fertilization to mediate their fast polyspermy block (Cross and Elinson, 1980; Grey et al., 1982; Webb and Nuccitelli, 1985; Glahn and Nuccitelli, 2003). We have recently demonstrated that the Ca^{2+}-activated Cl^- channel, TMEM16A, conducts this current in eggs from the African clawed frog *Xenopus laevis* (see Wozniak et al. in this issue). Although we know increased intracellular Ca^{2+} is necessary for the fast block, how fertilization signals increased Ca^{2+} to open TMEM16A channels was unknown. A prominent role for elevated intracellular Ca^{2+} as a trigger for the fast block has previously been demonstrated by two independent experiments. First, fertilization failed to evoke a depolarization in *X. laevis* eggs loaded with the Ca^{2+}-chelator BAPTA (Kline, 1988). Second, treating *X. laevis* eggs with a Ca^{2+} ionophore, a lipid-soluble compound that transports Ca^{2+} across the plasma membrane and increases the intracellular Ca^{2+} concentration, evoked a depolarization in the absence of fertilization (Grey et al., 1982). The ionophore-signaled depolarization demonstrated that increased intracellular Ca^{2+} is sufficient to trigger the fast block, and the BAPTA experiments demonstrated that an elevation of intracellular Ca^{2+} is necessary.

Here we sought to uncover the mechanisms by which fertilization signals increased intracellular Ca^{2+} in the *X. laevis* egg to activate the fast block. We reasoned that fertilization could signal the opening of Ca^{2+}-permeant channels to allow Ca^{2+} entry into the egg or that Ca^{2+} could be released from an intracellular store. To distinguish between these two possibilities, we interrogated existing proteomics and RNA-sequencing (RNA-seq) data and found that two Ca^{2+}-permeant channels, TrpV4 and PKD2, are expressed in *X. laevis* eggs (Wühr et al., 2014; Session et al., 2016). However, insemination in the presence of broad-spectrum Ca^{2+} channel inhibitors, at concentrations known to block the candidate channels, did not alter the fertilization-signaled depolarization. In contrast, inhibition of PLC and inositol 1,4,5-triphosphate (IP_3) receptors (IP_3Rs) on the ER successfully abolished any fertilization-signaled depolarization and increased the incidence of polyspermic fertilizations. Together these results indicate that fertilization activates PLC to release Ca^{2+} from the ER and signal the fast polyspermy block in *X. laevis*.

Table 2. **Development assays in various conditions**

	Undeveloped	Developed	Polyspermic	*n*
	%	%	%	
Control	3 ± 2	97 ± 2	13 ± 3	6
10 µM Gd	5 ± 5	95 ± 5	10 ± 7	3
20 µM SK&F 96365	23 ± 11	77 ± 11	16 ± 7	3
Control	46 ± 15	54 ± 15	13 ± 4	3
500 nM Xestospongin C	32 ± 8	68 ± 8	34 ± 6	3
Control	6 ± 5	94 ± 5	8 ± 4	3
100 µM 2-APB	19 ± 10	81 ± 10	69 ± 17	3
Control	18 ± 9	82 ± 9	11 ± 7	3
1 µM U73343	26 ± 16	74 ± 16	12 ± 3	3
1 µM U73122	35 ± 13	65 ± 13	60 ± 11	3

Mean ± SEM are reported. Out of the zygotes that initiated embryonic development, embryos were categorized as monospermic or polyspermic based on cleavage furrow symmetry. Control development for Xestospongin C was MR/3 with 2% DMSO.

Materials and methods

Reagents

Xestospongin C, $GdCl_3$, U-73343, and 2-aminoethoxydiphenyl borate (2-APB) were purchased from Tocris, and human chorionic gonadotropin was purchased from Henry Schien. U-73122 hydrate was purchased from Sigma-Aldrich. SK&F-96365 was purchased from Cayman Chemical. All other materials, unless noted, were purchased from Thermo Fisher Scientific.

Solutions

Variations of modified Ringer's (MR) solution were used for all experiments. MR contains (in mM) 100 NaCl, 1.8 KCl, 2.0 $CaCl_2$,

1.0 $MgCl_2$, and 5.0 HEPES, pH 7.8, and was filtered using a sterile, 0.2-µm polystyrene filter (Heasman et al., 1991).

Fertilization solution

Control fertilization recordings were made in our standard solution of 20% MR diluted in DDH_2O (also known as MR/5). Various inhibitors were added to MR/5 and used during fertilization recordings. Experimental conditions were made by diluting concentrated inhibitor stocks solutions, which were themselves made in water or DMSO. All recordings were made in solutions that contained a final DMSO concentration of <0.5%, except for those made in 500 nM Xestospongin C. The 500 nM Xestospongin C in MR/5 solution contained 2% DMSO; because we have found that fertilization in ≥2% DMSO alone can alter embryonic development (Tables 1 and 2), the control for the Xestospongin C treatment was MR/5 with 2% DMSO.

Solutions for embryonic development and polyspermy assays

Incidence of embryonic development and polyspermy were assayed in 33% MR (also known as MR/3). Various inhibitors were added to MR/3, which contained final DMSO concentrations of <0.5%, except for the 500-nM Xestospongin C trials. As described above, the 500-nM Xestospongin C treatment solution contained 2% DMSO; thus, we included MR/3 with 2% DMSO as a control solution for this trial.

Animals

All animal procedures were conducted using accepted standards of humane animal care and were approved by the Animal Care and Use Committee at the University of Pittsburgh. *X. laevis* adults were obtained commercially (Research Resource Identifier NXR_0.0031; NASCO) and housed at 18°C with a 12-h/12-h light/dark cycle.

Collection of gametes, fertilization, and developmental assays

As previously described (Wozniak et al., 2017), eggs were collected from sexually mature *X. laevis* females. In brief, females were injected 1,000 IU of human chorionic gonadotropin into their dorsal lymph sac and housed overnight for 12–16 h at 14–16°C. Within 2 h of being moved to room temperature, females began laying eggs, which were collected on dry Petri dishes. Eggs were then used within 10 min of being laid.

Sperm were collected from testes of *X. laevis* sexually mature males after euthanasia by a 30-min immersion in 3.6 g/liter tricaine-S (pH 7.4; Wozniak et al., 2017). Testes were manually cleaned by removing fat and vessels and were stored at 4°C in MR for usage on the day of dissection or in L-15 medium for use up to 1 wk later. For whole-cell recordings, sperm suspensions were created by mincing ∼1/10 of a testis in MR/5; if not used immediately, this solution was stored on ice and used within 1 h. No more than three separate sperm additions were added to an egg during a whole-cell recording, and the total added sperm suspension volume never exceeded 7.5% of the recording-solution volume. After insemination during whole-cell recordings, eggs were transferred to MR/3 for up to 16 h to monitor development.

Initiation of embryonic development and the incidence of polyspermy were assessed as previously described (Grey et al., 1982).

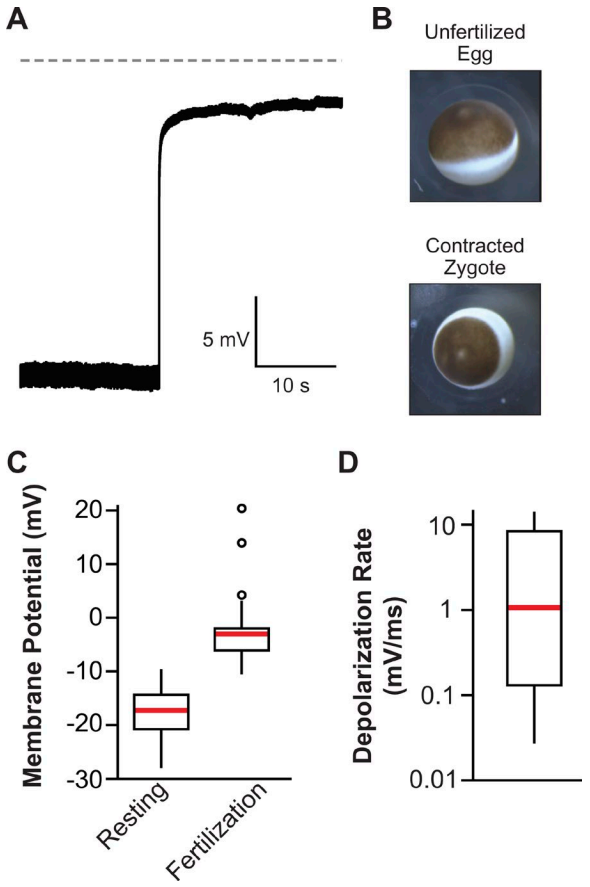

Figure 1. **Fertilization signals a depolarization in *X. laevis* eggs. (A)** Representative whole-cell recordings made during fertilization in control conditions (in MR/5 solution). Dashed line denotes 0 mV. **(B)** Images of *X. laevis* (top) egg before sperm addition and (bottom) egg ∼15 min after fertilization with animal pole contracted. Tukey box plot distributions of the (C) resting and fertilization potentials in control conditions and (D) depolarization rate (n = 31, recorded over 22 experiment days). The central line represents the median value, the box denotes the data spread from 25 and 75%, and the whiskers reflect 10–90%.

Approximately 20–40 eggs were placed in each treatment and incubated for 10 min before fertilization. Sperm were then minced in 1/10 testis in MR, and the sperm suspension was used to fertilize eggs. Approximately 90 min after insemination, the initiation of embryonic development was assessed based on the appearance of cleavage furrows. Polyspermic fertilization was determined based on the incidence of asymmetric and incomplete cleavage furrows during the first few cleavage events, whereas monospermic fertilization was noted based on symmetric, complete furrows.

Electrophysiology

Whole-cell recordings were made using TEV-200A amplifiers (Dagan) and digitized by Axon Digidata 1550A (Molecular Devices). The pClamp Software (Molecular Devices) was used for data acquisition at a rate of 5 kHz. Pipettes of 5–20 MΩ resistance were pulled from borosilicate glass and filled with 1 M KCl. Resting and fertilization potentials were generally stable and quantified ∼10 s before and after the depolarization, respectively. Depolarization rates were quantified by determining the maximum velocity of a 1-mV shift in the membrane potential for each recording.

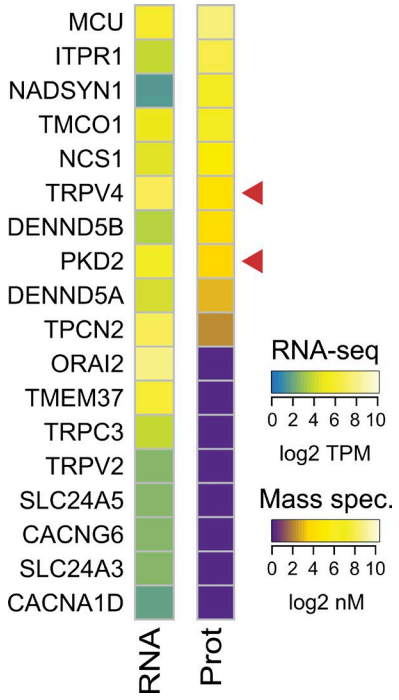

Figure 2. **Expression of Ca^{2+} channels in *X. laevis* eggs.** Heatmaps of RNA (left) and protein (Prot; right) expression levels of Ca^{2+} channels whose transcript levels were >1 TPM. Transcript levels (shown as TPM) were obtained from Session et al. (2016). Protein concentrations are from Wühr et al. (2014) as determined by mass spectrometry (mass spec.)–based proteomics in $\log_2$ nanomolar. Red arrows highlight plasma membrane localized Ca^{2+} channels found in eggs.

Imaging

Unfertilized and fertilized eggs were imaged with a stereoscope (Leica Microsystems) equipped with a Leica 10447157 1X objective and DFC310 FX camera. Images were analyzed using LAS (version 3.6.0 build 488) software and Photoshop (Adobe).

Proteomic and RNA-seq analysis

RNA-seq reads from Session et al. (2016) were downloaded from the NCBI Sequence Read Archive (accession no. SRX1287707). Reads were aligned using HISAT2 (Kim et al., 2015) with default parameters in paired-end mode to the *X. laevis* v9.1 genome (http://www.xenbase.org). Gene counts were obtained using featureCounts (Liao et al., 2014) on Xenbase primary gene models v1.8.3.2 in unstranded, paired-end mode using the gene_ID attribute and allowing multimappers (-p -s 0 -M). Raw counts were then normalized to transcripts per million. Expression values for L and S versions of each gene were summed.

To identify Ca^{2+}-permeant channels, we extracted all genes annotated with Gene Ontology (GO) molecular function terms that contained the keywords "calcium" and "channel" (Dataset S1) using Xenbase GO term annotations. Because of incomplete annotation of the *X. laevis* genes, GO terms associated with *Xenopus tropicalis* genes were transferred to their *X. laevis* orthologues. Heatmaps were generated in R Studio-1.1.383 using the heatmap.2 command from the gplots package.

To estimate the number of IP_3Rs in the egg, we combined the mass spectrometry–derived protein concentrations from Wühr et al. (2014) with the stoichiometry of the functional channel: four subunits of ITPR1 for each functional channel (Ludtke et al., 2011; Murray et al., 2013). We then assumed that *X. laevis* eggs are spherical and calculated their volume based on their measured diameter of 1.4 mm (Wozniak et al., 2017).

Quantification and statistical analyses

Igor (WaveMetrics) and Excel (Microsoft) software were used for analysis of electrophysiology recordings. Data from whole-cell recordings experiments are displayed with Tukey box plot distributions, where the box contains the data between 25 and 75%, the central line denotes the median, and the whiskers extend out to 10 and 90%. Additionally, for each experimental condition, the mean values ± SEM are reported (Table 1). Depolarization rates were $\log_{10}$ transformed before statistical analysis. *T* tests (one tailed for depolarization rates and two tailed for resting and fertilization potentials) were used to determine differences between fertilization treatments. Data from embryonic development assays are presented as mean values ± SEM (Table 2). ANOVAs followed by post hoc Holm–Bonferroni tests were used to compare each inhibitor treatment with the control for polyspermy assays, unless otherwise indicated.

Online supplemental material

The following materials are included in the supplement: Dataset 1 lists GO terms used to identify Ca^{2+} channels; RNA-seq data are from Session et al. (2016), and proteomics data are from Wühr et al. (2014) of Ca^{2+} channels in *X. laevis* eggs. Fig. S1 shows RNA and protein expression of Ca^{2+} channels in *X. laevis* eggs.

Results

Fertilization signals a depolarization in *X. laevis* eggs

To characterize the fast block to polyspermy, we made whole-cell recordings from *X. laevis* eggs during fertilization in control conditions (the MR/5 solution; see Materials and methods). Eggs with stable resting potentials were inseminated by pipetting the sperm suspension into the recording chamber directly above the egg. The eggs' membrane potentials were recorded for up to 40 min (Fig. 1 A) or until the cortex contracted (Fig. 1 B), an early indicator of successful fertilization. Fig. 1 A depicts a typical fertilization-evoked depolarization. A mean of 5.2 ± 0.5 min (n = 31) passed between sperm addition and the recorded depolarization of the fast block, which likely represents the time required for the sperm to penetrate the viscous jelly coat of the egg (Table 1; Glahn and Nuccitelli, 2003). Under control conditions, the mean egg resting potential was −17.9 ± 0.9 mV, and the fertilization potential was −2.6 ± 1.1 mV (n = 31; Fig. 1 C and Table 1). The mean rate of depolarization for eggs fertilized under the control conditions was 3.9 ± 0.8 mV/ms (n = 31; Fig. 1 D and Table 1).

Ca^{2+} entry into the egg is not required for the fast block in *X. laevis*

To identify the source of Ca^{2+} that signals the fast block, we first explored the hypothesis that fertilization may evoke Ca^{2+} entry from the extracellular environment through plasma membrane-traversing Ca^{2+} channels. We interrogated existing pro-

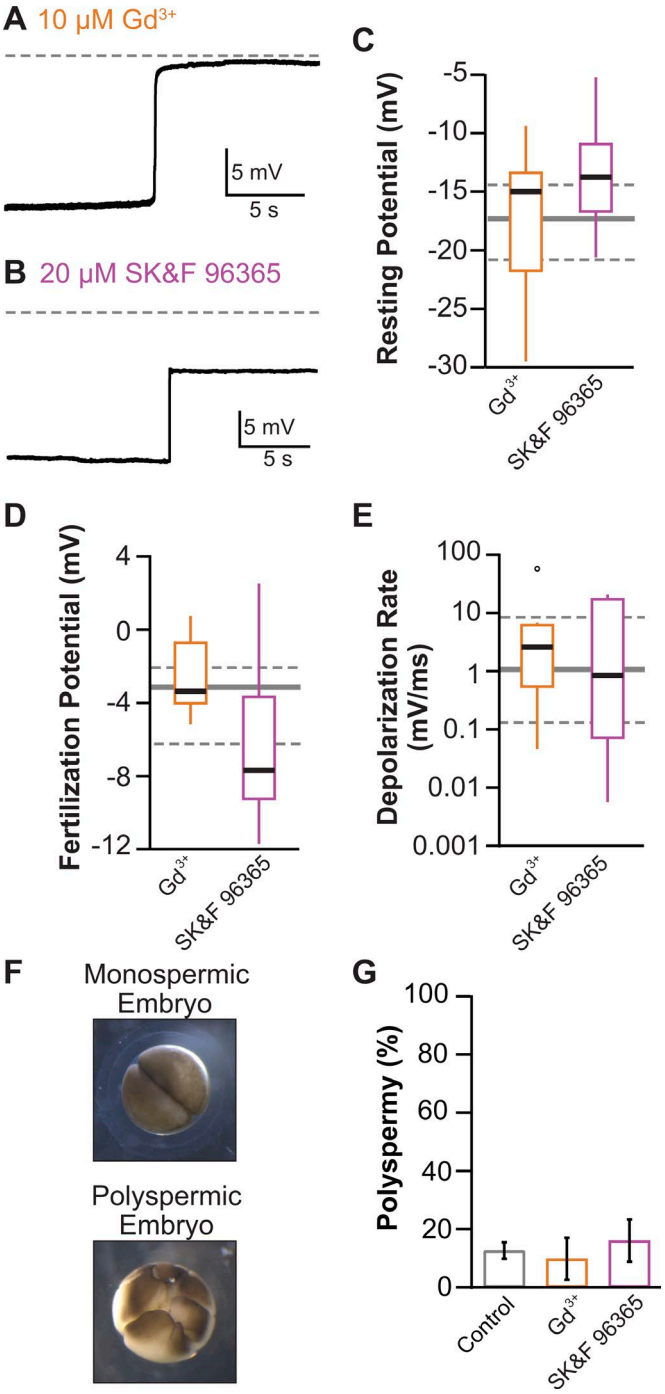

Figure 3. **Fertilization-signaled depolarization does not require Ca^{2+} entry into *X. laevis* eggs. (A and B)** Representative fertilization recordings made in solutions with 10 μM $GdCl_3$ (A) and 20 μM SK&F-96365 (B). Dashed lines denote 0 mV. **(C–E)** Tukey box plot distributions of the resting (C) and fertilization (D) potentials and depolarization rate (E) for indicated treatments (n = 8–12, recorded over 3 experiment days per treatment). In D and E, the gray lines denote the Tukey box plot distributions for recordings made in control conditions (in the MR/5 solution), where the solid line represents the median value, the dashed lines denote the data spread from 25 and 75%, and the whiskers reflect 10–90%. **(F)** Images of *X. laevis* embryos from monospermic (top) and polyspermic (bottom) fertilizations. **(G)** Proportion of polyspermic embryos out of total developed embryos in control, Gd^{3+}, and SK&F-96365 (n = 3–6, recorded over 3–6 experiment days per treatment, the mean values ± SEM are reported).

teomics and RNA-seq datasets and identified 49 Ca^{2+}-selective channels annotated in the *X. laevis* genome (Fig. S1 and Dataset S1). Out of the 18 transcripts that were expressed ≥1 transcript per million (TPM), proteomics detected 10 of these proteins in the *X. laevis* egg (Fig. 2; Wühr et al., 2014; Session et al., 2016). Of these 10 proteins, 4 were intracellular Ca^{2+} channels and transporters, including the IP_3 receptor type 1 and the mitochondrial Ca^{2+} uniporter (ITPR1, MCU, TMCO1, and TPCN2; Sakuntabhai et al., 1999; Bobe et al., 2004; Zhang et al., 2005; Berridge, 2009; Calcraft et al., 2009; Pitt et al., 2010; De Stefani et al., 2011; Wang et al., 2016; Sun et al., 2018). We also found four proteins that are not pore forming, although they are capable of regulating Ca^{2+} channel activity: the soluble Ca^{2+}-binding protein called frequinin (encoded by NCS1; Bourne et al., 2001; Nakamura et al., 2001), two guanine nucleotide exchange factors (DENND5A and DENND5B), and the NAD synthase 1 (NADSYN1). The final two proteins were the transient receptor potential subfamily V, member 4 (TrpV4) channel, and polycystin-2 (PKD2); these were the only candidates that conduct Ca^{2+} entry from the extracellular environment into the egg. The proteomics and RNA-seq data reveal that fertilization could open a membrane Ca^{2+} channel to increase intracellular Ca^{2+} and signal the fast block.

Next, we determined whether Ca^{2+} entry is required for the fast block by recording from *X. laevis* eggs inseminated in the presence of broad-spectrum inhibitors known to inhibit most Ca^{2+}-permeant channels including TrpV4 and PKD2: Gd^{3+} (González-Perrett et al., 2001; Suzuki et al., 2003) or SK&F-96365 (Clapham, 2007; Ho et al., 2012). There were no significant differences between depolarizations recorded under control conditions (Fig. 1) and in solutions supplemented with 10 μM $GdCl_3$ or 20 μM SK&F-96365 (Fig. 3, A and B; and Table 1). Like eggs fertilized under control conditions, the mean resting potential of eggs in Gd^{3+} was −17.0 ± 2.3 mV, and the fertilization potential was −2.6 ± 0.7 mV (n = 8; Fig. 3, C and D; and Table 1). The depolarization rate for eggs inseminated in Gd^{3+} was 10.6 ± 7.9 mV/ms (n = 8; Fig. 3 E and Table 1), compared with 3.9 ± 0.8 mV/ms in control conditions (n = 31; Fig. 1 C). Eggs recorded in SK&F-96365 had mean resting potentials of −13.6 ± 2.0 mV and depolarized to −6.4 ± 1.9 mV (n = 6; Fig. 3, C and D; and Table 1). The rate of depolarization of these eggs was 6.1 ± 3.7 mV/ms (Fig. 3 E and Table 1).

To further confirm that extracellular Ca^{2+} is not needed for the fast block, we quantified the incidence of polyspermy in eggs inseminated in Gd^{3+} and SK&F-96365. Polyspermic fertilization results in incomplete and asymmetric furrows during the first few cleavage events, whereas monospermy leads to symmetric furrows (Fig. 3 F; Grey et al., 1982). Blocking extracellular Ca^{2+} from entering eggs had no effect on polyspermy rates (Fig. 3 G and Table 2). Persistence of normal fertilization-evoked depolarizations and normal cleavage furrow formation in eggs inseminated with Ca^{2+} channel blockers demonstrates that Ca^{2+} entry from the extracellular environment is not required for the fast block.

The fast block requires IP_3-evoked Ca^{2+} release from the ER

To explore whether Ca^{2+} release from an intracellular store activates the fast block, we first interrogated an IP_3-mediated pathway. We reasoned that several minutes after fertilization, an increase of IP_3 in the egg is known to initiate the slow block

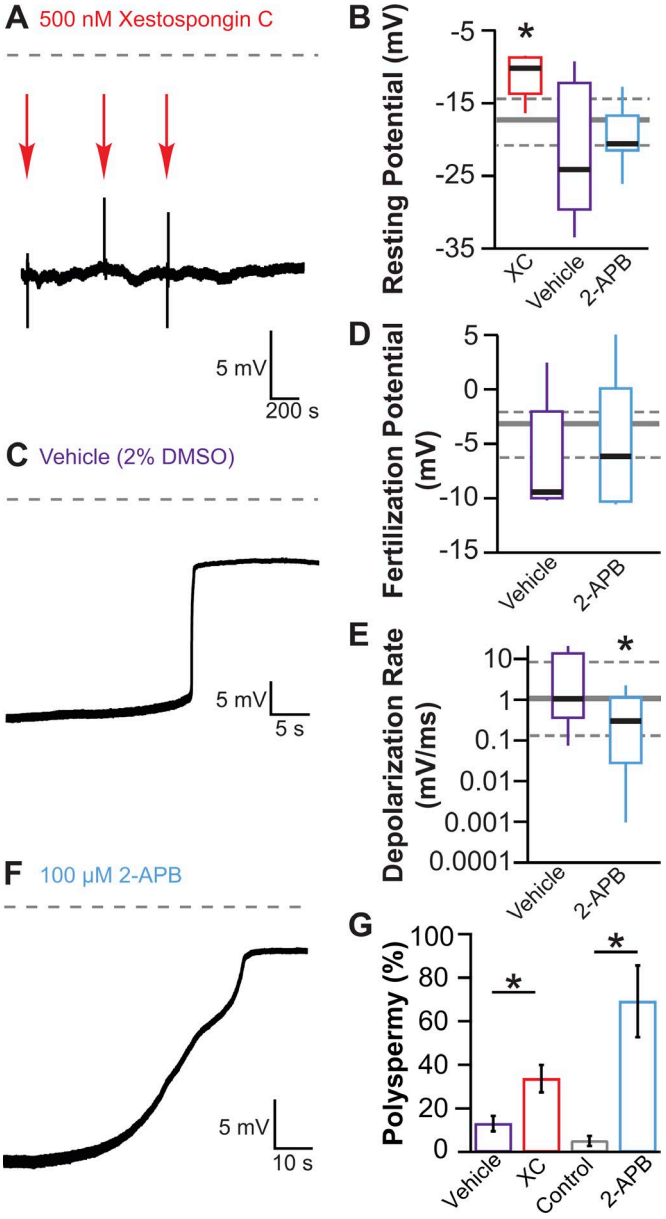

Figure 4. **ER-released Ca^{2+} is essential for the fast polyspermy block.** Representative fertilization recordings made in the presence of 500 nM Xestospongin C (XC; A), vehicle (2% DMSO; C), or 100 µM 2-APB (F). Dashed line denotes 0 mV, and arrows indicate sperm additions. Tukey box plot distributions of the resting (B) and fertilization (D) potentials, as well as the depolarization rates (E), from recordings made in the indicated treatments (n = 5–8, 2–4 experiment days per treatment). In B and D, the gray lines behind the box plots represent the Tukey box plot distributions for the control (MR/5) data, where the solid line represents the median value, the dashed lines denote the data spread from 25 and 75%, and the whiskers reflect 10–90%. **(G)** Proportion of polyspermic embryos out of total developed embryos in vehicle (2% DMSO in MR/5), Xestospongin C, control (MR/5), and 2-APB (n = 3, recorded over 3 experiment days per treatment, the mean values ± SEM are reported). *, P < 0.05.

by signaling Ca^{2+} release from the ER to initiate cortical granule exocytosis (Sato et al., 2006). Additionally, injecting *X. laevis* eggs with an IP_3R antibody inhibits this Ca^{2+} wave and ceases development (Runft et al., 1999). Together, these studies indicate that IP_3 is necessary for early signaling events in *X. laevis* eggs. Furthermore, our own bioinformatic analysis substantiates the presence of the IP_3R (encoded by the ITPR1 gene) in *X. laevis* eggs (Fig. 2). Based on protein concentrations, we estimate that the *X. laevis* egg includes ~5.3×10^{10} IP_3Rs. Although IP_3Rs are abundant in the *X. laevis* egg, it was unclear whether fertilization could evoke a fast-enough elevation of IP_3 to trigger the fast block. We therefore determined whether blocking the IP_3R altered the fertilization-signaled depolarization, as well as the incidence of polyspermy.

In the presence of the potent IP_3R inhibitor, Xestospongin C (Gafni et al., 1997; Kanki et al., 2001), fertilization failed to evoke any depolarization in five independent trials (Fig. 4 A), yet all five of these embryos developed cleavage furrows. The resting potential of eggs in 500 nM Xestospongin C was elevated compared with the control, −11.0 ± 1.4 mV in Xestospongin C (n = 5) versus −21.5 ± 4.2 mV in MR/5 with 2% DMSO (P < 0.05, t test; Fig. 4 B and Table 1). Others have shown that most eggs held at −11 mV are capable of fertilization and the initiation of embryonic development (Glahn and Nuccitelli, 2003). Because our Xestospongin C treatment included 2% DMSO, we controlled for these experiments by inseminating eggs in vehicle alone (2% DMSO in MR/5; Fig. 4 C and Table 1). We found that the biophysical properties of the fast block recorded from eggs inseminated in vehicle alone were not different from control recordings made in vehicle alone, including the mean depolarization rate in eggs inseminated in 2% DMSO (5.8 ± 3.9 mV/ms, n = 5), which was statistically indistinguishable from control depolarizations (P > 0.05, t test; Fig. 4, B, D, and E; and Table 1). Inhibition of the fertilization-signaled depolarization by Xestospongin C thereby demonstrates that the IP_3R mediate the depolarization of the egg.

In the presence of 2-APB (Maruyama et al., 1997), a less-potent IP_3R inhibitor, fertilization evoked slower depolarizations compared with recordings made under the control conditions (Fig. 4, E and F; and Table 1). Specifically, fertilization of eggs inseminated in 100 µM 2-APB depolarized at a rate of 0.6 ± 0.3 mV/ms (n = 8) compared with 3.9 ± 0.8 mV/ms (n = 31) in MR/5 (P < 0.05, t test). The depolarization rate is directly proportional to the number of TMEM16A channels opened by fertilization (Wozniak et al., 2018). Therefore, a slower depolarization rate in 2-APB reflects an attenuated Ca^{2+} release from the ER to ultimately open fewer TMEM16A channels. Based on rates measured in the presence and absence of 2-APB, we estimate that fertilization opened 6.5-fold fewer TMEM16A channels in the presence of the drug.

Insemination of eggs in either Xestospongin C or 2-APB led to a significant increase in the incidence of polyspermy compared with their controls (Fig. 3 G and Table 2). For example, 500 nM Xestospongin C led to 34 ± 6% polyspermy compared with 13 ± 4% in 2% DMSO (t test, P < 0.01; Fig. 3 G and Table 2). Overall, blockade of the IP_3R with either Xestospongin C or 2-APB diminished the fast block and increased the incidence of polyspermy. Together, these data demonstrate that an IP_3-evoked Ca^{2+} release from the ER is essential for the fast block.

The fast block requires PLC

IP_3 is generated de novo by the enzymatic activity of PLC, whereby the membrane phospholipid phosphatidylinositol 4,5-bisphosphate (PIP_2) is cleaved into IP_3 and diacylglycerol. To

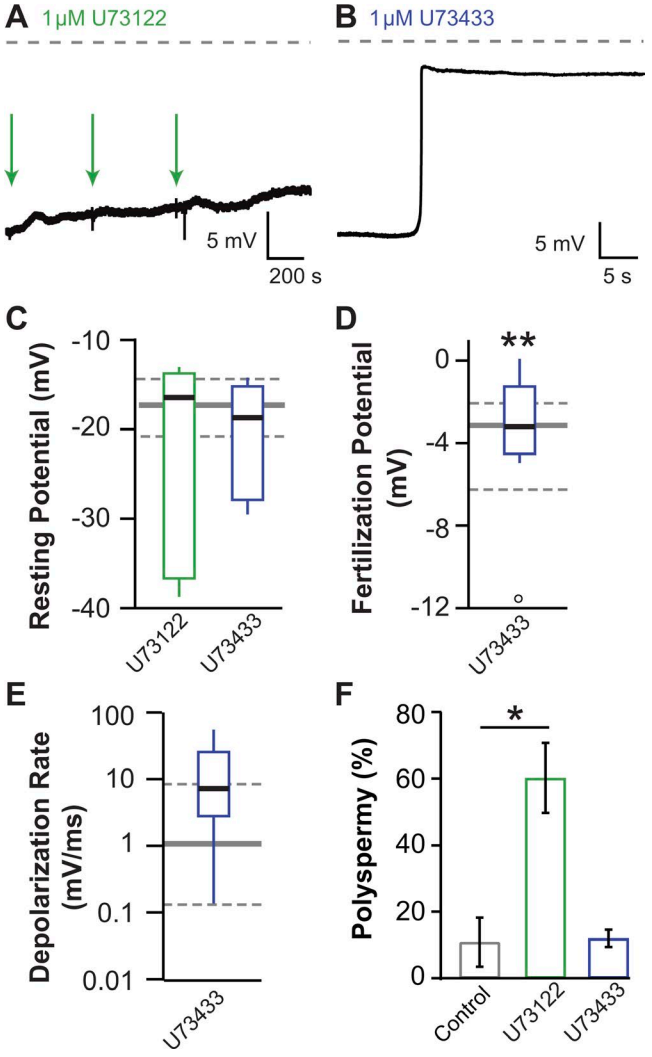

Figure 5. **PLC is required for the fast block. (A and B)** Representative fertilization recordings made in 1 μM U73122 (A) or 1 μM U73343 (B). Dashed line denotes 0 mV, and arrows indicate sperm additions. **(C–E)** Tukey box plot distributions of the resting (C) and fertilization (D) potentials and the depolarization rates (E) made in indicated treatments (n = 7–8, recorded over 3–5 experiment days per treatment, the mean values ± SEM are reported). The gray lines behind the box plots represent the Tukey box plot distributions for the control (MR/5) data, where the solid line represents the median value and the dashed lines denote the data spread from 25 and 75% and the whiskers reflect 10–90%. **(F)** Percent polyspermic embryos out of total developed embryos in control (MR/5), U73122, and U73343. *, P < 0.05; **, P < 0.01.

determine whether fertilization activates the synthesis of IP_3, we inseminated eggs in the presence of the PLC inhibitor U73122 or its inactive analogue U73343 (Bleasdale et al., 1990; Jin et al., 1994). In seven separate trials, fertilization failed to evoke any depolarization in eggs inseminated in 1 μM U73122 (Fig. 5 A). Normal depolarizations, however, were recorded in the presence of 1 μM of the inactive analogue U73343 (n = 8; Fig. 5 B). Neither the resting nor the fertilization potentials recorded in U73122 and U73343 were different from those recorded in the MR/5 solution (P > 0.05, t test; Fig. 5, C and D). Unexpectedly, eggs inseminated in the inactive analogue depolarized more quickly relative to control fertilizations at a rate of 14.9 ± 6.6 mV/ms (P < 0.05, t test; Fig. 5 E).

We found that eggs inseminated in U73122 had a significantly higher incidence of polyspermy than control (Fig. 5 F): 60 ± 11% (n = 3) polyspermy with U73122 versus 11 ± 7% (n = 3) in control conditions (ANOVA, P < 0.01). In contrast, the incidence of polyspermy in U73343 was the same as control (ANOVA, P > 0.05). Together these data suggest that the enzymatic activity of PLC, which generates IP_3, is required to initiate the fast block.

Discussion

Despite the widespread use of the fast polyspermy block by evolutionarily divergent species, the signaling pathways that underlie these fertilization-evoked depolarizations have remained elusive. Here we sought to uncover the source of Ca^{2+} that initiates this pathway in *X. laevis*. Our data demonstrate that the fast block is signaled by activation of PLC, to increase IP_3 and activate the ER-localized IP_3R (Fig. 6). Release of Ca^{2+} from the ER then opens TMEM16A channels to depolarize the egg as part of the fast polyspermy block (Fig. 6; Wozniak et al., 2018).

Previous studies showed that fertilization-evoked depolarization varies with respect to amplitude and shape, even when recorded under control conditions (Cross and Elinson, 1980; Grey et al., 1982; Webb and Nuccitelli, 1985). Our study further demonstrates that the rate of depolarization varies for each unique fertilization event. Because the depolarization rate is directly proportional to the number of TMEM16A channels that open (Wozniak et al., 2018), our data imply that different fertilization events lead to the opening of different numbers of channels. The variance in numbers of TMEM16A channels activated by response to fertilization may reflect varying amounts of Ca^{2+} released from the ER in different eggs. For example, if fertilization opens TMEM16A by a pathway that involves receptor activation and second-messenger signaling, variation may reveal that some sperm activate multiple receptors, whereas other sperm may activate only one receptor.

To uncover the source of Ca^{2+} that signals the fast block, we first explored whether Ca^{2+}-permeant channels on the eggs' plasma membranes were required for this fertilization-signaled depolarization. We have recently demonstrated that the jelly layer surrounding *X. laevis* eggs is enriched with 6.3 mM freely diffusing Ca^{2+} (Wozniak et al., 2017), thereby indicating that fertilization could signal Ca^{2+} entry even with changing environmental conditions. By mining existing proteomics and RNA-seq datasets (Wühr et al., 2014; Session et al., 2016), we uncovered that *X. laevis* eggs express two Ca^{2+}-permeant channels, TrpV4 and PKD2 (Fig. 2). A possible role for either channel in the fast block was attractive because both are known to transduce physical stress into cationic currents (Delmas, 2005; Toft-Bertelsen et al., 2017), and sperm–egg fusion at fertilization theoretically exerts forces on the membrane of the egg that could trigger the fast block. We found, however, that fertilization evoked normal depolarizations in the presence of the broad-spectrum Ca^{2+} channel inhibitors Gd^{3+} or SK&F-96365 known to block both TrpV4 (Suzuki et al., 2003; Ho et al., 2012) and PKD2 (Ho et al., 2012; Fig. 3). These results reveal that Ca^{2+} entry into the egg is unessential for the fast block, a surprising finding given that Ca^{2+} enters eggs from other external fertilizers at fertilization to ini-

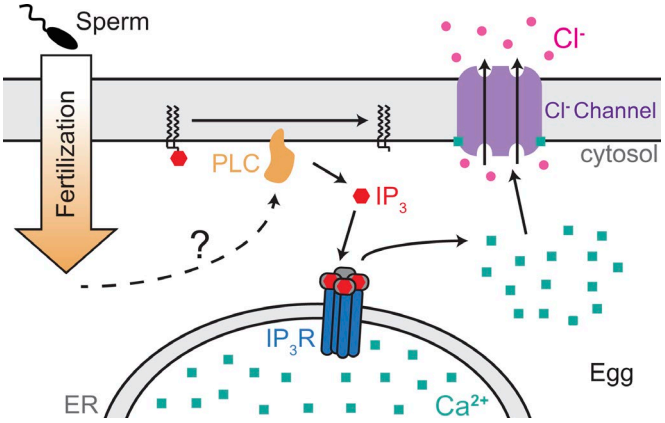

Figure 6. **Model for the fast polyspermy block in *X. laevis*.** In the fast block to polyspermy in *X. laevis* eggs, fertilization activates a PLC, which then cleaves PIP_2 to create IP_3. This increased IP_3 then activates its cognate receptor on the ER to evoke a Ca^{2+} release. This ER-derived Ca^{2+} then activates a Cl^- channel, which conducts a Cl^- efflux to depolarize the egg. Research described in the companion paper (Wozniak et al., 2018) identifies this Cl^- channel as TMEM16A. This fertilization-signaled depolarization prevents sperm entry into an already-fertilized egg.

tiate the fast block. In starfish, for example, the depolarization of the fast block is driven by a nicotinic acid–adenine dinucleotide phosphate–activated, SK&F-96365 and verapamil–sensitive Ca^{2+} channel (Moccia et al., 2004).

To explore a possible role for Ca^{2+} release from an intracellular store in the fast block, we tested the hypothesis that Ca^{2+} release from the ER via IP_3R was required for the fertilization-evoked depolarization. A prominent role for an IP_3-signaled Ca^{2+} release from the ER was particularly attractive because *X. laevis* eggs lack other prominent ER Ca^{2+} signaling mechanisms, such as ryanodine receptors (Fig. S1; Parys et al., 1992; Petersen and Berridge, 1994). Moreover, in eggs from nearly all species examined thus far, fertilization increases the IP_3 content to activate Ca^{2+} release from the ER and signal the cortical granule exocytosis of the slow block to polyspermy (Gould and Stephano, 1991; Kume et al., 1993; Stricker et al., 1994; Stricker, 1999). Yet, because the slow polyspermy block occurs minutes after sperm entry (Stricker, 1999; Wong and Wessel, 2006) we worried that using a second messenger cascade would be too slow for the fast block. To test whether IP_3 signals the fast block, we inseminated *X. laevis* eggs in the presence of IP_3R inhibitors Xestospongin C or 2-APB. We found that inhibition of the IP_3R diminished the fast block and increased the incidence of polyspermy (Fig. 4). These results demonstrate that IP_3 signals both the fast and the slow blocks to polyspermy in *X. laevis*. Furthermore, other intracellular Ca^{2+} stores, such as mitochondria or lysosomes, are not sufficient to induce the fast block in the absence of IP_3-mediated Ca^{2+} release from the ER.

Finally, we explored a possible role for PLC in signaling the fast block. Theoretically, sperm could bypass the need for PLC activity by entering eggs preloaded with IP_3 necessary for the fast block. However, fertilization failed to depolarize *X. laevis* eggs in the presence of the broad-spectrum PLC inhibitor U73122 (Fig. 5; Bleasdale et al., 1990). In contrast, depolarizations were unaltered in eggs inseminated in the presence of the U73122 inactive analogue, U73343 (Fig. 5; Bleasdale et al., 1990). Together these results demonstrate a requirement for PLC activity for the fast block and reveal that IP_3 is created de novo.

Although the fast block is limited to externally fertilizing organisms, the slow polyspermy block is ubiquitous in all sexual reproducers (Stricker, 1999; Wong and Wessel, 2006). The enzymatic activity of PLC is needed for the slow block of all animals studied thus far; however, the PLC isoform responsible differs. For the slow block in mammals, the sperm releases the soluble PLC type zeta (PLCζ) as it enters the egg (Cox et al., 2002; Saunders et al., 2002; Nozawa et al., 2018). In *X. laevis*, the slow block is activated by sperm binding to uroplakins on the plasma membrane of the egg (Sato et al., 2006) to induce a tyrosine phosphorylation cascade that activates the membrane-anchored PLCγ (Sato et al., 2000). Whether the same tyrosine phosphorylation cascade that activates PLCγ to signal the slow block in *X. laevis* eggs also activates the fast block is yet to be determined. *X. laevis* eggs contain PLC isoforms β and γ (Wühr et al., 2014), which can both be blocked by U73122 (Bleasdale et al., 1990). A principle difference between PLC enzymes is the mechanism of their activation. Whereas PLCγ is activated by tyrosine phosphorylation, the PLCβ isoform is activated by G-protein–coupled receptors. The subtype that mediates the fast block in *X. laevis* is yet to be determined.

In summary, fertilization quickly activates PLC to generate the IP_3 needed to induce ER Ca^{2+} release. This pathway culminates in a depolarizing efflux of Cl^- from the channel TMEM16A (Wozniak et al., 2018), thereby resulting in the fast polyspermy block in *X. laevis*. Many questions remain regarding the upstream components of this pathway. For example, do sperm activate the depolarization by binding to a receptor on the extracellular surface of the egg, or is sperm entry into the egg required? How does egg membrane depolarization prevent sperm entry? Answering these questions will not only reveal the first events of new life but will also uncover the voltage dependence of fertilization.

Acknowledgments

We thank Z. Crowell, D.O. Beleny, M.A. Napolitano, and B.L. Mayfield for excellent technical assistance. We thank L. Jaffe and K. Kiselyov for helpful discussions and advice.

This work was supported by an Andrew W. Mellon Foundation Predoctoral Fellowship to K.L. Wozniak, the March of Dimes Foundation Basil O'Connor grant 5-FY16-307 to M.T. Lee, and National Institutes of Health grant R00HD69410 to A.E. Carlson.

The authors declare no competing financial interests.

Author contributions: K.L. Wozniak, M.T. Lee, and A.E. Carlson conceived of the research. K.L. Wozniak, W.A. Phelps, M. Tembo, M.T. Lee, and A.E. Carlson created the experiments, designed their implementation, planned analyses, and wrote the manuscript.

Merritt C. Maduke served as editor.

Submitted: 16 March 2018
Accepted: 12 June 2018

References

Berridge, M.J. 2009. Inositol trisphosphate and calcium signalling mechanisms. *Biochim. Biophys. Acta.* 1793:933–940. https://doi.org/10.1016/j.bbamcr.2008.10.005

Bleasdale, J.E., N.R. Thakur, R.S. Gremban, G.L. Bundy, F.A. Fitzpatrick, R.J. Smith, and S. Bunting. 1990. Selective inhibition of receptor-coupled phospholipase C-dependent processes in human platelets and polymorphonuclear neutrophils. *J. Pharmacol. Exp. Ther.* 255:756–768.

Bobe, R., R. Bredoux, E. Corvazier, J.P. Andersen, J.D. Clausen, L. Dode, T. Kovács, and J. Enouf. 2004. Identification, expression, function, and localization of a novel (sixth) isoform of the human sarco/endoplasmic reticulum Ca2+ATPase 3 gene. *J. Biol. Chem.* 279:24297–24306. https://doi.org/10.1074/jbc.M314286200

Bourne, Y., J. Dannenberg, V. Pollmann, P. Marchot, and O. Pongs. 2001. Immunocytochemical localization and crystal structure of human frequenin (neuronal calcium sensor 1). *J. Biol. Chem.* 276:11949–11955. https://doi.org/10.1074/jbc.M009373200

Brawley, S.H. 1991. The fast block against polyspermy in fucoid algae is an electrical block. *Dev. Biol.* 144:94–106. https://doi.org/10.1016/0012-1606(91)90482-I

Calcraft, P.J., M. Ruas, Z. Pan, X. Cheng, A. Arredouani, X. Hao, J. Tang, K. Rietdorf, L. Teboul, K.T. Chuang, et al. 2009. NAADP mobilizes calcium from acidic organelles through two-pore channels. *Nature.* 459:596–600. https://doi.org/10.1038/nature08030

Charbonneau, M., M. Moreau, B. Picheral, J.P. Vilain, and P. Guerrier. 1983. Fertilization of amphibian eggs: A comparison of electrical responses between anurans and urodeles. *Dev. Biol.* 98:304–318. https://doi.org/10.1016/0012-1606(83)90361-5

Clapham, D.E. 2007. SnapShot: Mammalian TRP channels. *Cell.* 129:220. https://doi.org/10.1016/j.cell.2007.03.034

Cox, L.J., M.G. Larman, C.M. Saunders, K. Hashimoto, K. Swann, and F.A. Lai. 2002. Sperm phospholipase Czeta from humans and cynomolgus monkeys triggers Ca2+ oscillations, activation and development of mouse oocytes. *Reproduction.* 124:611–623. https://doi.org/10.1530/rep.0.1240611

Cross, N.L., and R.P. Elinson. 1980. A fast block to polyspermy in frogs mediated by changes in the membrane potential. *Dev. Biol.* 75:187–198. https://doi.org/10.1016/0012-1606(80)90154-2

Delmas, P. 2005. Polycystins: Polymodal receptor/ion-channel cellular sensors. *Pflugers Arch.* 451:264–276. https://doi.org/10.1007/s00424-005-1431-5

De Stefani, D., A. Raffaello, E. Teardo, I. Szabò, and R. Rizzuto. 2011. A forty-kilodalton protein of the inner membrane is the mitochondrial calcium uniporter. *Nature.* 476:336–340. https://doi.org/10.1038/nature10230

Gafni, J., J.A. Munsch, T.H. Lam, M.C. Catlin, L.G. Costa, T.F. Molinski, and I.N. Pessah. 1997. Xestospongins: Potent membrane permeable blockers of the inositol 1,4,5-trisphosphate receptor. *Neuron.* 19:723–733. https://doi.org/10.1016/S0896-6273(00)80384-0

Glahn, D., and R. Nuccitelli. 2003. Voltage-clamp study of the activation currents and fast block to polyspermy in the egg of *Xenopus laevis*. *Dev. Growth Differ.* 45:187–197. https://doi.org/10.1034/j.1600-0854.2004.00684.x

González-Perrett, S., K. Kim, C. Ibarra, A.E. Damiano, E. Zotta, M. Batelli, P.C. Harris, I.L. Reisin, M.A. Arnaout, and H.F. Cantiello. 2001. Polycystin-2, the protein mutated in autosomal dominant polycystic kidney disease (ADPKD), is a Ca2+-permeable nonselective cation channel. *Proc. Natl. Acad. Sci. USA.* 98:1182–1187. https://doi.org/10.1073/pnas.98.3.1182

Gould, M.C., and J.L. Stephano. 1991. Peptides from sperm acrosomal protein that initiate egg development. *Dev. Biol.* 146:509–518. https://doi.org/10.1016/0012-1606(91)90252-X

Gould-Somero, M., L.A. Jaffe, and L.Z. Holland. 1979. Electrically mediated fast polyspermy block in eggs of the marine worm, *Urechis caupo*. *J. Cell Biol.* 82:426–440. https://doi.org/10.1083/jcb.82.2.426

Grey, R.D., M.J. Bastiani, D.J. Webb, and E.R. Schertel. 1982. An electrical block is required to prevent polyspermy in eggs fertilized by natural mating of *Xenopus laevis*. *Dev. Biol.* 89:475–484. https://doi.org/10.1016/0012-1606(82)90335-9

Heasman, J., S. Holwill, and C.C. Wylie. 1991. Fertilization of cultured *Xenopus* oocytes and use in studies of maternally inherited molecules. *Methods Cell Biol.* 36:213–230. https://doi.org/10.1016/S0091-679X(08)60279-4

Hille, B. 2001. Ion Channels of Excitable Membranes. Sinauer Associates, Inc., Sunderland, MA.

Ho, T.C., N.A. Horn, T. Huynh, L. Kelava, and J.B. Lansman. 2012. Evidence TRPV4 contributes to mechanosensitive ion channels in mouse skeletal muscle fibers. *Channels (Austin).* 6:246–254. https://doi.org/10.4161/chan.20719

Jaffe, L.A. 1976. Fast block to polyspermy in sea urchin eggs is electrically mediated. *Nature.* 261:68–71. https://doi.org/10.1038/261068a0

Jaffe, L.A., and M. Gould. 1985. Polyspermy-preventing mechanisms. *In* Biology of Fertilization. C.B. Metz and A. Monroy, editors. Academic Press Inc., Orlando, FL. 223–250. https://doi.org/10.1016/B978-0-12-492603-5.50012-8

Jaffe, L.A., N.L. Cross, and B. Picheral. 1983a. Studies of the voltage-dependent polyspermy block using cross-species fertilization of amphibians. *Dev. Biol.* 98:319–326. https://doi.org/10.1016/0012-1606(83)90362-7

Jaffe, L.A., A.P. Sharp, and D.P. Wolf. 1983b. Absence of an electrical polyspermy block in the mouse. *Dev. Biol.* 96:317–323. https://doi.org/10.1016/0012-1606(83)90168-9

Jin, W., T.M. Lo, H.H. Loh, and S.A. Thayer. 1994. U73122 inhibits phospholipase C-dependent calcium mobilization in neuronal cells. *Brain Res.* 642:237–243. https://doi.org/10.1016/0006-8993(94)90927-X

Kanki, H., M. Kinoshita, A. Akaike, M. Satoh, Y. Mori, and S. Kaneko. 2001. Activation of inositol 1,4,5-trisphosphate receptor is essential for the opening of mouse TRP5 channels. *Mol. Pharmacol.* 60:989–998. https://doi.org/10.1124/mol.60.5.989

Kim, D., B. Langmead, and S.L. Salzberg. 2015. HISAT: a fast spliced aligner with low memory requirements. *Nat. Methods.* 12:357–360. https://doi.org/10.1038/nmeth.3317

Kline, D. 1988. Calcium-dependent events at fertilization of the frog egg: Injection of a calcium buffer blocks ion channel opening, exocytosis, and formation of pronuclei. *Dev. Biol.* 126:346–361. https://doi.org/10.1016/0012-1606(88)90145-5

Kume, S., A. Muto, J. Aruga, T. Nakagawa, T. Michikawa, T. Furuichi, S. Nakade, H. Okano, and K. Mikoshiba. 1993. The *Xenopus* IP_3 receptor: Structure, function, and localization in oocytes and eggs. *Cell.* 73:555–570. https://doi.org/10.1016/0092-8674(93)90142-D

Liao, Y., G.K. Smyth, and W. Shi. 2014. featureCounts: an efficient general purpose program for assigning sequence reads to genomic features. *Bioinformatics.* 30:923–930. https://doi.org/10.1093/bioinformatics/btt656

Ludtke, S.J., T.P. Tran, Q.T. Ngo, V.Y. Moiseenkova-Bell, W. Chiu, and I.I. Serysheva. 2011. Flexible architecture of IP3R1 by Cryo-EM. *Structure.* 19:1192–1199. https://doi.org/10.1016/j.str.2011.05.003

Maruyama, T., T. Kanaji, S. Nakade, T. Kanno, and K. Mikoshiba. 1997. 2APB, 2-aminoethoxydiphenyl borate, a membrane-penetrable modulator of Ins(1,4,5)P3-induced Ca2+ release. *J. Biochem.* 122:498–505. https://doi.org/10.1093/oxfordjournals.jbchem.a021780

Miyazaki, S., and S. Hirai. 1979. Fast polyspermy block and activation potential: Correlated changes during oocyte maturation of a starfish. *Dev. Biol.* 70:327–340. https://doi.org/10.1016/0012-1606(79)90031-9

Moccia, F., D. Lim, K. Kyozuka, and L. Santella. 2004. NAADP triggers the fertilization potential in starfish oocytes. *Cell Calcium.* 36:515–524. https://doi.org/10.1016/j.ceca.2004.05.004

Murray, S.C., J. Flanagan, O.B. Popova, W. Chiu, S.J. Ludtke, and I.I. Serysheva. 2013. Validation of cryo-EM structure of IP_3R1 channel. *Structure.* 21:900–909. https://doi.org/10.1016/j.str.2013.04.016

Nakamura, T.Y., D.J. Pountney, A. Ozaita, S. Nandi, S. Ueda, B. Rudy, and W.A. Coetzee. 2001. A role for frequenin, a Ca2+-binding protein, as a regulator of Kv4 K+-currents. *Proc. Natl. Acad. Sci. USA.* 98:12808–12813. https://doi.org/10.1073/pnas.221168498

Nozawa, K., Y. Satouh, T. Fujimoto, A. Oji, and M. Ikawa. 2018. Sperm-borne phospholipase C zeta-1 ensures monospermic fertilization in mice. *Sci. Rep.* 8:1315. https://doi.org/10.1038/s41598-018-19497-6

Parys, J.B., S.W. Sernett, S. DeLisle, P.M. Snyder, M.J. Welsh, and K.P. Campbell. 1992. Isolation, characterization, and localization of the inositol 1,4,5-trisphosphate receptor protein in Xenopus laevis oocytes. *J. Biol. Chem.* 267:18776–18782.

Petersen, C.C., and M.J. Berridge. 1994. The regulation of capacitative calcium entry by calcium and protein kinase C in Xenopus oocytes. *J. Biol. Chem.* 269:32246–32253.

Pitt, S.J., T.M. Funnell, M. Sitsapesan, E. Venturi, K. Rietdorf, M. Ruas, A. Ganesan, R. Gosain, G.C. Churchill, M.X. Zhu, et al. 2010. TPC2 is a novel NAADP-sensitive Ca2+ release channel, operating as a dual sensor of luminal pH and Ca2+. *J. Biol. Chem.* 285:35039–35046. https://doi.org/10.1074/jbc.M110.156927

Runft, L.L., J. Watras, and L.A. Jaffe. 1999. Calcium release at fertilization of Xenopus eggs requires type I IP(3) receptors, but not SH2 domain-mediated activation of PLCgamma or G(q)-mediated activation of PLCbeta. *Dev. Biol.* 214:399–411. https://doi.org/10.1006/dbio.1999.9415

Sakuntabhai, A., V. Ruiz-Perez, S. Carter, N. Jacobsen, S. Burge, S. Monk, M. Smith, C.S. Munro, M. O'Donovan, N. Craddock, et al. 1999. Mutations in ATP2A2, encoding a Ca2+ pump, cause Darier disease. *Nat. Genet.* 21:271–277. https://doi.org/10.1038/6784

Sato, K., A.A. Tokmakov, T. Iwasaki, and Y. Fukami. 2000. Tyrosine kinase-dependent activation of phospholipase Cgamma is required for calcium transient in Xenopus egg fertilization. *Dev. Biol.* 224:453–469. https://doi.org/10.1006/dbio.2000.9782

Sato, K., Y. Fukami, and B.J. Stith. 2006. Signal transduction pathways leading to Ca2+ release in a vertebrate model system: Lessons from Xenopus eggs. *Semin. Cell Dev. Biol.* 17:285–292. https://doi.org/10.1016/j.semcdb.2006.02.008

Saunders, C.M., M.G. Larman, J. Parrington, L.J. Cox, J. Royse, L.M. Blayney, K. Swann, and F.A. Lai. 2002. PLC zeta: A sperm-specific trigger of Ca(2+) oscillations in eggs and embryo development. *Development.* 129:3533–3544.

Session, A.M., Y. Uno, T. Kwon, J.A. Chapman, A. Toyoda, S. Takahashi, A. Fukui, A. Hikosaka, A. Suzuki, M. Kondo, et al. 2016. Genome evolution in the allotetraploid frog Xenopus laevis. *Nature.* 538:336–343. https://doi.org/10.1038/nature19840

Stricker, S.A. 1999. Comparative biology of calcium signaling during fertilization and egg activation in animals. *Dev. Biol.* 211:157–176. https://doi.org/10.1006/dbio.1999.9340

Stricker, S.A., V.E. Centonze, and R.F. Melendez. 1994. Calcium dynamics during starfish oocyte maturation and fertilization. *Dev. Biol.* 166:34–58. https://doi.org/10.1006/dbio.1994.1295

Sun, Z., H. Zhang, X. Wang, Q.C. Wang, C. Zhang, J.Q. Wang, Y.H. Wang, C.Q. An, K.Y. Yang, Y. Wang, et al. 2018. TMCO1 is essential for ovarian follicle development by regulating ER Ca^{2+} store of granulosa cells. *Cell Death Differ.* https://doi.org/10.1038/s41418-018-0067-x

Suzuki, M., A. Mizuno, K. Kodaira, and M. Imai. 2003. Impaired pressure sensation in mice lacking TRPV4. *J. Biol. Chem.* 278:22664–22668. https://doi.org/10.1074/jbc.M302561200

Toft-Bertelsen, T.L., D. Križaj, and N. MacAulay. 2017. When size matters: Transient receptor potential vanilloid 4 channel as a volume-sensor rather than an osmo-sensor. *J. Physiol.* 595:3287–3302. https://doi.org/10.1113/JP274135

Wang, Q.C., Q. Zheng, H. Tan, B. Zhang, X. Li, Y. Yang, J. Yu, Y. Liu, H. Chai, X. Wang, et al. 2016. TMCO1 is an ER Ca(2+) load-activated Ca(2+) channel. *Cell.* 165:1454–1466. https://doi.org/10.1016/j.cell.2016.04.051

Webb, D.J., and R. Nuccitelli. 1985. Fertilization potential and electrical properties of the Xenopus laevis egg. *Dev. Biol.* 107:395–406. https://doi.org/10.1016/0012-1606(85)90321-5

Wong, J.L., and G.M. Wessel. 2006. Defending the zygote: Search for the ancestral animal block to polyspermy. *Curr. Top. Dev. Biol.* 72:1–151.

Wozniak, K.L., B.L. Mayfield, A.M. Duray, M. Tembo, D.O. Beleny, M.A. Napolitano, M.L. Sauer, B.W. Wisner, and A.E. Carlson. 2017. Extracellular Ca2+ is required for fertilization in the African clawed frog, *Xenopus laevis. PLoS One.* 12:e0170405. https://doi.org/10.1371/journal.pone.0170405

Wozniak, K.L., W.A. Phelps, M. Tembo, M.T. Lee, and A.E. Carlson. 2018. The TMEM16A channel mediates the fast polyspermy block in *Xenopus laevis. J. Gen. Physiol.* https://doi.org/10.1085/jgp.201812071

Wühr, M., R.M. Freeman Jr., M. Presler, M.E. Horb, L. Peshkin, S. Gygi, and M.W. Kirschner. 2014. Deep proteomics of the Xenopus laevis egg using an mRNA-derived reference database. *Curr. Biol.* 24:1467–1475. https://doi.org/10.1016/j.cub.2014.05.044

Zhang, S.L., Y. Yu, J. Roos, J.A. Kozak, T.J. Deerinck, M.H. Ellisman, K.A. Stauderman, and M.D. Cahalan. 2005. STIM1 is a Ca2+ sensor that activates CRAC channels and migrates from the Ca2+ store to the plasma membrane. *Nature.* 437:902–905. https://doi.org/10.1038/nature04147